LETTERS

Mesostructured germanium with cubic pore symmetry

Gerasimos S. Armatas[1] & Mercouri G. Kanatzidis[1]

Regular mesoporous oxide materials have been widely studied[1–8] and have a range of potential applications, such as catalysis, absorption and separation. They are not generally considered for their optical and electronic properties. Elemental semiconductors with nanopores running through them represent a different form of framework material with physical characteristics contrasting with those of the more conventional bulk, thin film and nanocrystalline forms[1]. Here we describe cubic mesostructured germanium, MSU-Ge-1, with gyroidal channels containing surfactant molecules, separated by amorphous walls that lie on the gyroid (G) minimal surface as in the mesoporous silica MCM-48 (ref. 2). Although Ge is a high-melting, covalent semiconductor that is difficult to prepare from solution polymerization, we succeeded in assembling a continuous Ge network using a suitable precursor for Ge^{4-} atoms. Our results indicate that elemental semiconductors from group 14 of the periodic table can be made to adopt mesostructured forms such as MSU-Ge-1, which features two three-dimensional labyrinthine tunnels obeying $Ia\bar{3}d$ space group symmetry and separated by a continuous germanium minimal surface that is otherwise amorphous. A consequence of this new structure for germanium, which has walls only one nanometre thick, is a wider electronic energy bandgap (1.4 eV versus 0.66 eV) than has crystalline or amorphous Ge. Controlled oxidation of MSU-Ge-1 creates a range of germanium suboxides with continuously varying Ge:O ratio and a smoothly increasing energy gap.

The liquid-crystal templating mechanism for achieving synthetic control on the nanoscale has led to the discovery of inorganic mesophases with remarkable pore architectures. This methodology involves electrostatic interactions and charge matching at the interface of the self-assembled surfactant molecules and inorganic species. Originally used with silica-based materials[2], this approach was extended to organosilicates[3,4] and transition metal oxides[5–8]. Whereas the mesoporous ceramic oxides are desirable for catalytic, separation and adsorption applications, their frameworks lack exciting electronic and optical properties. The idea of semiconducting mesoporous framework solids led various research groups to develop synthetic routes for non-oxidic materials by binding chalcogenide clusters with a variety of linkage metal ions[9–11]. These materials demonstrate long-range ordering with optoelectronic properties that originate from the surfactant/chalcogenide framework.

In contrast to mesostructured compounds, mesostructured elemental materials have not been developed and only a few examples involving transition-metal systems have been reported, including Pt and Pt/Ru alloys[12,13]. The synthesis of elemental structures perforated with tunnels on the nanoscale is challenging because of the difficulty in growing or organizing appropriate precursors in a desired manner. Elemental mesoporous semiconductors with a three-dimensional arrangement of pores could modulate their physical parameters in such a way that new opto-electronic properties not present in the bulk analogues can be achieved[9,14].

The semiconductor germanium, with its many technological applications, has been studied extensively[15–17]. A large number of different methods of synthesis and developing of Ge nanoparticles have been reported[18,19]. Recently, Ge nanocrystals prepared in the liquid phase using a non-anionic surfactant as the size- and shape-directing agent has been described[20,21]. Although the synthesis of germanium nanocrystals is well established, with procedures that affect the size and shape of the 'bulk' nanoparticles, no work has been reported for the synthesis of Ge semiconductors with mesostructured frameworks. Here we report a successful synthetic strategy for the preparation of a mesostructured Ge semiconductor, based on a liquid-crystal-templated technique and a new form of framework based entirely on Ge with a nanopore system of cubic gyroid symmetry.

To produce the mesostructured germanium, we used Ge^{4-} anions derived from Mg_2Ge and linked them via a metathesis reaction with germanium tetrachloride ($GeCl_4$) in the presence of cationic surfactants; see scheme (1). The synthesis must be carried out under an inert atmosphere. The amphilic surfactant *N*-eicosane-*N*-methyl-*N*,*N*-dis(2-hydroxyethyl)ammonium bromide (EMBHEAB) was used as the micellar template in formamide solution. The prepared hybrid organic–inorganic material labelled MSU-Ge-1 has the formula EMBHEA-$[Ge]_m$ (where $m \approx 8$):

$$[C_{20}H_{41}\text{-}N(CH_2CH_2OH)_2Me]Br + Mg_2Ge \xrightarrow[N_2\ \text{atmosphere}]{\text{formamide,}} \underset{\text{Organized micellar solution}}{\text{“}[C_{20}H_{41}\text{-}N(CH_2CH_2OH)_2Me]_x\{Ge^{4-}\}\text{”}} + MgBr_2 \xrightarrow{GeCl_4\ \text{linking agent}} \text{MSU-Ge-1} \quad (1)$$

The powder X-ray diffraction (XRD) pattern of MSU-Ge-1 is shown in Fig. 1a. The pattern exhibits several well-resolved peaks in the low-angle range $2\theta = 2$–$8°$, which can be indexed as (211), (220), (321), (400), (420), (332), (422), (431), (611) and (543) diffraction peaks; this pattern corresponds to the cubic $Ia\bar{3}d$ space group with a refined cubic unit-cell parameter of $a = 8.4$ nm. The large number of observed Bragg peaks in the XRD pattern indicates a high pore order and long-range periodicity in the structure. Furthermore, the XRD results reveal that the framework of germanium maps onto the gyroidal minimal surface, analogous to that of the mesoporous silicate MCM-48 (Fig. 1b)[22].

The chemical composition of MSU-Ge-1 was determined with elemental C,H,N and energy-dispersive microprobe analysis. The analysis confirmed the presence of Ge only and the absence of any Mg or halide element (Cl or Br); see Fig. 1c. The composition of MSU-Ge-1 was consistent with the stoichiometry of EMBHEA-$[Ge]_8$.

[1]Department of Chemistry, Michigan State University, East Lansing, Michigan 48824, USA.

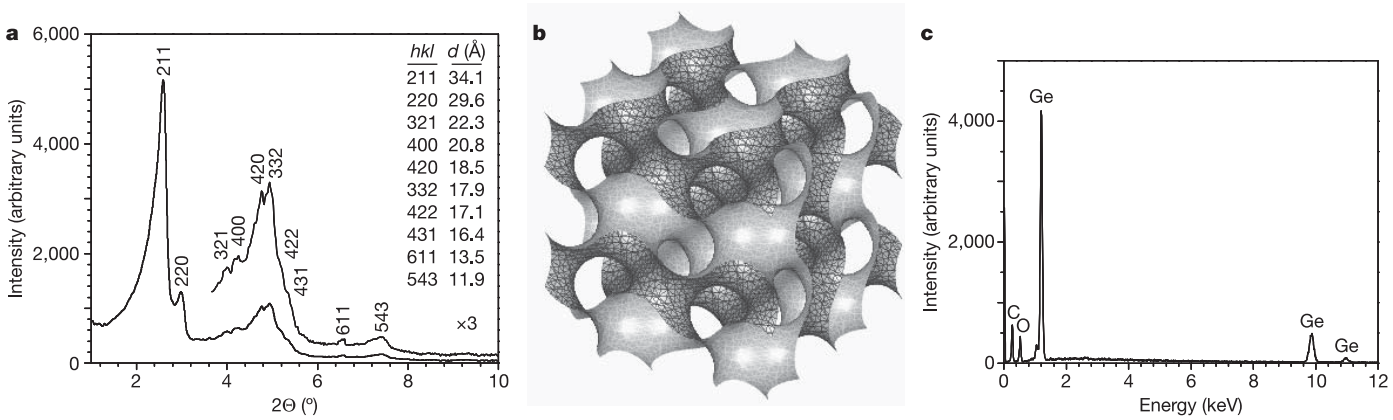

Figure 1 | 1 X-ray scattering of mesostructured MSU-Ge-1, bicontinuous gyroid minimal surface and energy-dispersive X-ray spectrum. a, Powder XRD pattern of cubic mesostructured germanium. This pattern is similar to those reported for high-quality cubic silica MCM-48 systems. The indexing of the Bragg reflections (see inset) is consistent with a body-centred unit cell with $a = 8.4$ nm. **b**, The bi-continuous gyroid minimal surface with $Ia\bar{3}d$ pore symmetry. The elemental germanium framework follows the gyroid surface and the molecules of surfactant occupy the pore channels. The two different shades of surface belong to the two independent channel systems in the structure. **c**, Energy-dispersive X-ray spectrum of purified MSU-Ge-1 showing the present of only Ge element. The carbon- and oxygen-related peaks are attributed to the surfactant in the material and possibly the grid.

Figure 2 presents typical transmission electron microscopy (TEM) images obtained from MSU-Ge-1, and the corresponding fast Fourier transforms (FFT) taken along a thin area of the images. We succeeded in recording TEM images along the [100], [110], [111] and [311] directions, which revealed regular and extended pore periodicity confirming that the material is a cubic gyroidal mesostructure[21]. Furthermore, indexing of the diffraction spots of FFTs (insets in Fig. 2) confirms that the periodic structure is defined by body-centred-cubic symmetry in the $Ia\bar{3}d$ space group. From the TEM studies, the size of the surfactant and the XRD-determined pore–pore spacings we estimate a Ge wall thickness of ~1 nm.

The absence of Bragg peaks in the higher-angle region ($2\theta > 10°$) of the XRD pattern establish the non-periodic structure of the Ge framework in MSU-Ge-1. However, the local structure of the framework was probed with X-ray diffuse scattering and pair distribution function (PDF) analysis[23]. Figure 3a shows the PDF plots as a function of interatomic distance r for MSU-Ge-1 and polycrystalline germanium. The PDF plot exhibits strong interatomic correlation

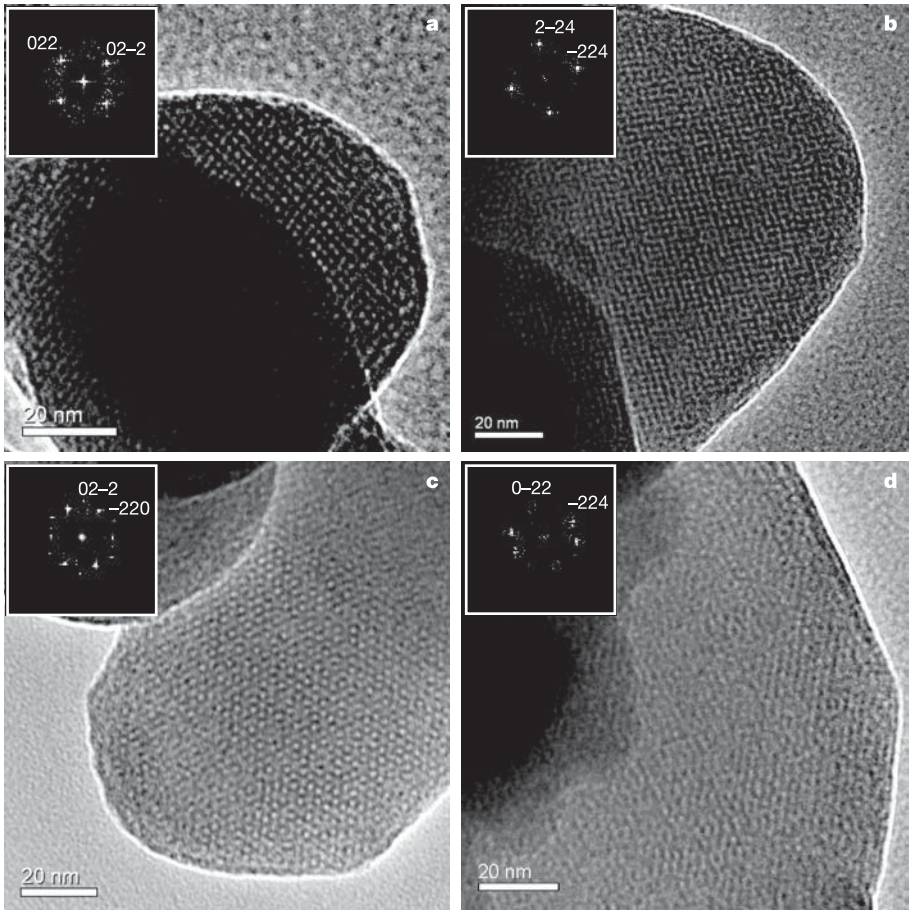

Figure 2 | TEM images of mesoporous germanium semiconductor MSU-Ge-1. a, Image taken along the [100] direction; **b**, along the [110] direction; **c**, along the [111] direction and **d**, along the [311] direction. The pore–pore spacings are consistent with those deduced from XRD. Insets in each panel show FFT images taken along an area of the high-resolution TEM images.

vectors at 2.3 and 4.0 Å, which correspond to Ge–Ge bonds and Ge···Ge next-nearest-neighbour distances in the mesoporous framework. By comparison, polycrystalline Ge (Fig. 3a) and amorphous Ge[24] shows the same two correlation peaks at 2.4 and 4.0 Å originating from the Ge–Ge bonds and Ge···Ge second-neighbour distances and indicating local structure similar to that of MSU-Ge-1. This suggests that the MSU-Ge-1 framework has a well-defined local structure (that is, Ge–Ge bonding); however, because of the very thin walls (~1 nm) of the gyroid Ge network we expect most of the Ge atoms to be located on the surface. Therefore, we cannot be sure that the full tetrahedral geometry of crystalline or amorphous Ge is in fact present in MSU-Ge-1. The lack of the atomic pair correlation peaks at distances beyond 5 Å confirms the absence of intermediate or long-range order in the Ge network of MSU-Ge-1. Crystalline Ge exhibits longer-range interatomic correlation peaks owing to its periodicity. Importantly, the PDF lacks correlation peaks at 1.7 and 3.2 Å, which would arise from Ge–O bonds and Ge–O–Ge moieties in the structure[25].

Although oxide species in the mesostructured framework of MSU-Ge-1 are not expected on the basis of the anaerobic conditions of scheme (1), their presence was probed with Fourier transform infrared (FTIR) spectroscopy. FTIR spectroscopy is sensitive to atom–atom vibrations and the characteristic band can be identified even if a small amount of Ge–O bonds existed in the structure. The spectrum of the as-prepared semiconductor indicated a lack of stretching vibrations at 904 and 956 cm^{-1} that is typical of Ge–O bonding. This supports the PDF analysis results discussed above. Evidence for oxide species (GeO_x) on the germanium framework began to appear in samples after extended exposure (over 2 days) to air, judging from the growth of the intense and broad Ge–O band centred at 924 cm^{-1} (see Fig. 3b).

The mesostructured germanium framework of MSU-Ge-1 exhibits optical and electrical properties different from those of the bulk crystalline or amorphous phases. Figure 3c shows the optical absorption spectra of the as-prepared MSU-Ge-1 and crystalline Ge as well as those obtained after extended exposure of MSU-Ge-1 to ambient air (over 10 h and 2 days). There is a clear and substantial blueshift of the absorption edge in MSU-Ge-1 relative to bulk Ge by ~0.76 eV. That is, the absorption associated with the bandgap transition occurs at 1.42 eV for MSU-Ge-1 versus 0.66 eV for Ge. This marked blueshift can be understood by considering the changes in the density of the electronic energy states due to the thin walls of the Ge network in MSU-Ge-1 (~1 nm). We observed similar blueshifted bandgaps of ~1.4 eV in Ge nanocrystals ~4 nm in diameter—a consequence of quantum size effects[26].

The gradual bandgap increase in the oxidation products of MSU-Ge-1 (Fig. 3c) suggests the generation of novel sub-oxide GeO_x species in the framework. The formation of GeO_x causes a successive widening of the energy gap involving the conversion of Ge–Ge bonds to Ge–O–Ge moieties. This was confirmed by PDF of the air-oxidized species, which shows correlation peaks at 1.8, 2.9 and 4.2 Å (see Supplementary Fig. S1). These are interatomic correlations from Ge–O bonds, Ge···Ge second neighbours (via the Ge–O–Ge moieties) and Ge···Ge distant neighbours (see Supplementary Fig. S1). The end stage of this process is presumably GeO_2 which has a bandgap of 4.56 eV. The continuous blueshift with degree of oxidation indicates a homogeneous process and an evolution from Ge to GeO_x, and not a generation of a mixture of MSU-Ge-1 and GeO_2 phases. The controlled air oxidation of MSU-Ge-1 is topotactic (as judged by the XRD patterns of air-oxidized sample which indicate retention of the gyroid and the $Ia\bar{3}d$ space group; see Supplementary Fig. S2) and leads to a mesostructured material. Therefore the range of GeO_x compositions generated in this fashion represents a novel class of materials worthy of future studies of its own.

The thermal stability of MSU-Ge-1 was examined with thermogravimetric (TGA) and differential TGA analysis in a nitrogen atmosphere (Fig. 3d). The TGA profile shows a weight loss (14%) below 250 °C occurring in broad steps due to removal of physisorbed and possibly chemisorbed formamide. This is followed by a gradual weight loss of 42.5% occurring between 250 and 460 °C, which corresponds to the decomposition of surfactants that fill the mesopores. The material obtained at 600 °C was shown to be crystalline Ge.

Mesoporous semiconductors should be a fertile ground for physicochemical investigations[27]. Application possibilities may arise now

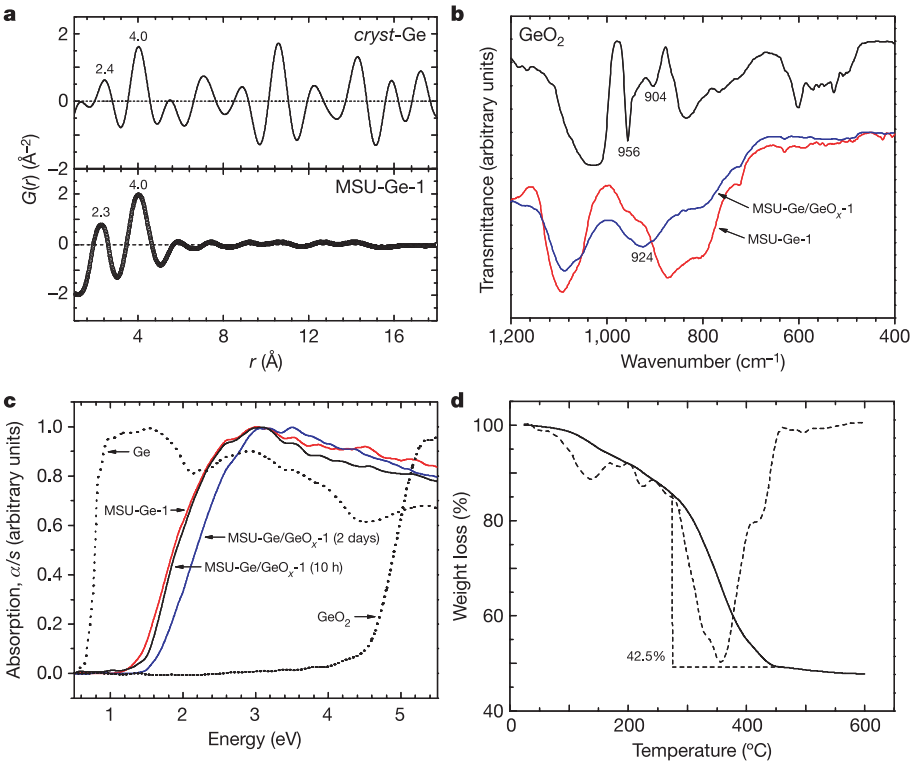

Figure 3 | PDF analysis, FTIR and optical absorption spectra and TGA data. a, Reduced atomic PDF $G(r)$ as a function of the interatomic distance r of mesostructured Ge and microcrystalline Ge (*cryst*-Ge) materials. Amorphous Ge shows a similar $G(r)$ function to that of MSU-Ge-1 (ref. 24). **b**, FTIR spectra of MSU-Ge-1 (red line), and the sample after extended exposure in the air (~2 days) (blue line) as well as crystalline GeO_2. The intense peak centred at 924 cm^{-1} of the oxidized MSU-Ge-1 material is attributed to broadening of the Ge–O vibration bands at 904 and 956 cm^{-1} (all spectra were recorded in diffuse reflectance mode). **c**, Optical absorption spectra of MSU-Ge-1 (red line) and oxidized material after 10 h exposure (black line) and after 2 days exposure to air (blue line). The results reveal energy bandgap 1.42, 1.47 and 1.61 eV for the MSU-Ge-1 and oxidized versions, respectively. The absorption spectra of bulk microcrystalline Ge (0.66 eV) and GeO_2 (4.56 eV) are also given for comparison. (α and S are the absorption and scattering coefficients, respectively.) **d**, TGA profile of as-prepared elemental mesoporous germanium (under nitrogen flow of 20 ml min^{-1}). The weight loss 42.5% in the temperature range 250–460 °C, indicated from the differential TGA curve (dashed line), we attribute to the combustion of surfactant.

that we can study and exploit the semiconducting properties of the Ge network, and in a broader sense those of mesoporous materials based on elements. Moreover, the approach of using elemental Zintl anions (as in Mg_2Ge) as a template seems particularly suited to constructing a wide range of elemental porous materials—and could generate a class of mesostructured elements with novel combinations of properties, such as medium or narrow energy gaps, light absorption properties or dopability. We have also found (work to be published elsewhere) that a mesoporous germanium network of the MCM-41 type constructed from Ge-clusters can also be made by a surfactant-templated process. These observations open up the possibility of general synthetic routes to ordered mesoporous elements with a variety of pore architectures, including mesoporous silicon.

METHODS

Preparation of Mg_2Ge precursor and cationic surfactant. The Zintl compound Mg_2Ge was prepared according to a modified literature preparation[28], inside a glovebox under nitrogen atmosphere. Ge powder and Mg metal with 10% molar excess were heated at 650 °C for 3 days in a sealed Nd tube, enclosed in an evacuated silica ampoule. The purity of the blue-grey product was confirmed with powder XRD. The amphiphilic surfactant EMBHEAB was prepared by reacting stoichiometric amounts of 1-bromoeicosaene with *N*-methyldiethenolamine in ethanol under reflux conditions for 48 h. Pure surfactant compound was obtained by recrystallizing twice from $CHCl_3$–ethyl acetate mixture solution[29].

Preparation of MSU-Ge-1. A typical procedure for the preparation of MSU-Ge-1 is as follows: finely ground powder of Mg_2Ge (48 mg, 0.04 mmol) was suspended in 5 ml formamide at 75 °C under continuous stirring for 18 h. The mixture was allowed to cool to 65 °C and the surfactant (280 mg, 0.06 mmol) was added. The mixture was stirred for 5 h and heated slowly to 75 °C. A solution of 0.04 mmol $GeCl_4$ in 1 ml of formamide was then added dropwise to this mixture using a pipette and the resulting mixture was aged overnight at 85 °C (the $GeCl_4$ solution must be added immediately upon preparation within a period of approximately 2 min). The light brown-grey product was isolated by filtration, washed with warm formamide several times and dried under vacuum at room temperature overnight to yield MSU-Ge-1 in ~83% yield. All manipulations were carried out in a glovebox filled with nitrogen. To remove any dense Ge phase the as-prepared material was suspended in chloroform (1 mg ml^{-1}) while stirring for 20 min. The less-dense MSU-Ge-1 forms a stable suspension whereas the minor byproducts sink. The suspension was decanted carefully with a pipette and the pure product was isolated after filtration, washed with chloroform and dried under vacuum at room temperature for 12 h.

Elemental C,H,N analysis was performed in a Perkin Elmer Series II CHNS/O Analyser 2400 instrument. The sample was heated at 160 °C for 1 h under N_2 flow before the measurements. The results were consistent from sample to sample and the average was C 32.24%, H 5.97%, and N 1.61%.

Attempts to remove the surfactant from mesostructured germanium by thermal decomposition led to contraction of the inorganic framework with consequent loss of pore ordering. For example, heating at 400 °C for 3 days, although it removes most of the surfactant (only 8% remains), leads to a shrinkage of the unit-cell volume by 19% and lowering of the pore periodicity. The specific surface area on such thermally treated material was found to be 18 m^2 g^{-1} by nitrogen adsorption measurements. The thermal treatment was as follows: the samples were heated from 30 to 230 °C (5° min^{-1}) for 3 h and then from 230 to 400 °C (5° min^{-1}) for 3 days under a nitrogen flow of 30 ml min^{-1}.

Received 3 February; accepted 24 April 2006.

1. Ozin, G. A. Nanomaterials—endosemiconductors and exosemiconductors. *Mater. Chem. Adv. Chem. Ser.* **245,** 335–371 (1995).
2. Kresge, C. T., Leonowicz, M. E., Roth, W. J., Vartuli, J. C. & Beck, J. S. Ordered mesoporous molecular sieves synthesized by a liquid-crystal template mechanism. *Nature* **359,** 710–712 (1992).
3. Asefa, T. *et al.* Periodic mesoporous organosilicas with organic groups inside the channel walls. *Nature* **402,** 867–871 (1999).
4. Inagaki, S., Guan, S., Ohsuna, T. & Terasaki, O. An ordered mesoporous organosilica hybrid material with a crystal-like wall structure. *Nature* **416,** 304–307 (2002).
5. Tian, Z.-R. *et al.* Manganese oxide mesoporous structures: mixed-valent semiconducting catalysts. *Science* **276,** 926–930 (1997).
6. Antonelli, D. M. & Ying, J. Y. Synthesis of a stable hexagonally packed mesoporous niobium oxide molecular sieve through a novel ligand-assisted templating mechanism. *Angew. Chem. Int. Edn Engl.* **35,** 426–430 (1996).
7. Lu, Q., Gao, F., Li, Y., Zhou, Y. & Zhao, D. Synthesis of germanium oxide mesoporous with a new intermediate state. *Micropor. Mesopor. Mater.* **56,** 219–225 (2002).
8. Zou, X., Conradsson, T., Klingstedt, M., Dadachov, M. S. & O'Keeffe, M. A mesoporous germanium oxide with crystalline pore walls and its chiral derivative. *Nature* **437,** 716–719 (2005).
9. MacLachlan, M. J., Coombs, N. & Ozin, G. A. Non-aqueous supramolecular assembly of mesostructured metal germanium sulphides from $(Ge_4S_{10})^{4-}$ clusters. *Nature* **397,** 681–684 (1999).
10. Trikalitis, P. N., Rangan, K. K., Bakas, T. & Kanatzidis, M. G. Varied pore organization in mesostructured semiconductors based on the $[SnSe_4]^{4-}$ anion. *Nature* **410,** 671–675 (2001).
11. Rangan, K. K., Trikalitis, P. N. & Kanatzidis, M. G. Light-emitting mesostructured sulfides with hexagonal symmetry: supramolecular assembly of $[Ge_4S_{10}]^{4-}$ clusters with trivalent metal ions and cetylpyridinium surfactant. *J. Am. Chem. Soc.* **122,** 10230–10231 (2000).
12. Attard, G. S. *et al.* Mesoporous platinum films from lyotropic liquid crystalline phases. *Science* **278,** 838–840 (1997).
13. Attard, G. S. *et al.* Liquid-crystal templates for nanostructured metals. *Angew. Chem. Int. Edn Engl.* **36,** 1315–1317 (1997).
14. Mohanan, J. L., Arachchige, I. U. & Brock, S. L. Porous semiconductor chalcogenide aerogels. *Science* **307,** 397–400 (2005).
15. Dunlap, W. C. Intrinsic conductivity of germanium. *Science* **112,** 419–420 (1950).
16. Bundy, F. P. & Kasper, J. S. A new dense form of solid germanium. *Science* **139,** 340–342 (1963).
17. Tauc, J., Grigorov, R. & Vancu, A. Optical properties and electronic structure of amorphous germanium. *Phys. Status Solidi (b)* **15,** 627–637 (1966).
18. Gerion, D. *et al.* Solution synthesis of germanium nanocrystals: success and open challenges. *Nano Lett.* **4,** 597–602 (2004).
19. Taylor, B. R., Kauzlarich, S. M., Lee, H. W. H. & Delgado, G. R. Solution synthesis and characterization of quantum confined Ge nanoparticles. *Chem. Mater.* **11,** 2493–2500 (1999).
20. Das, A. K., Kamila, J. & Dev, B. N. Self-assembled Ge nanostructures on polymer-coated silicon: Growth and characterization. *Appl. Phys. Lett.* **77,** 951–953 (2000).
21. Zhu, Y., Yuan, C. L. & Ong, P. P. Enhancement of photoluminescence in Ge nanoparticles by neighboring amorphous C in composite Ge/C thin films. *J. Appl. Phys.* **93,** 6029–6033 (2003).
22. Alfredsson, V. & Anderson, M. W. Structure of MCM-48 revealed by transmission electron microscopy. *Chem. Mater.* **8,** 1141–1146 (1996).
23. Billinge, S. J. L. & Kanatzidis, M. G. Beyond crystallography: the study of disorder, nanocrystallinity and crystallographically challenged materials with pair distribution functions. *Chem. Commun.* **7,** 749–760 (2004).
24. Temkin, R. J., Paul, W. & Connell, G. A. N. Amorphous germanium. Structural properties. *Adv. Phys.* **22,** 581–641 (1973).
25. Price, D. L. & Saboungi, M.-L. Structure of vitreous germania. *Phys. Rev. Lett.* **81,** 3207–3210 (1998).
26. Nakamura, Y., Watanabe, K., Fukuzawa, Y. & Ichikawa, M. Observation of the quantum-confinement effect in individual Ge nanocrystals on oxidized Si substrates using scanning tunneling spectroscopy. *Appl. Phys. Lett.* **87,** 133119 (2005).
27. Davis, M. E. Ordered porous materials for emerging applications. *Nature* **417,** 813–821 (2002).
28. Klemm, W. & Westlinning, Z. Untersuchungen über die Verbindungen des Magnesiums mit den Elementen der IV b-Gruppe. *Z. Anorg. Allg. Chem.* **245,** 365–380 (1941).
29. Broxon, T. J. & Chung, R. P.-T. Micellar bound meisenheimer complexes. *J. Org. Chem.* **55,** 3886–3890 (1990).

Supplementary Information is linked to the online version of the paper at www.nature.com/nature.

Acknowledgements We thank C. Malliakas for his help with the PDF data processing. We thank the National Science Foundation for financial support.

Author Information Reprints and permissions information is available at npg.nature.com/reprintsandpermissions. The authors declare no competing financial interests. Correspondence and requests for materials should be addressed to M.G.K. (kanatzid@cem.msu.edu).